

## Radiative Electron Capture to Continuum (RECC) and the Short-Wavelength Limit of Electron- Nucleus Bremsstrahlung in near-relativistic Collisions

S. Hagmann<sup>1,2</sup>, M. Nofal<sup>1,2,3</sup>, Th. Stöhlker<sup>2</sup>, D.H. Jakubassa-Amundsen<sup>4</sup>, Ch. Kozhuharov<sup>2</sup>, X. Wang<sup>5</sup>, A. Gumberidze<sup>2</sup>, U. Spillmann<sup>2</sup>, R. Reuschl<sup>2</sup>, S. Hess<sup>2</sup>, S. Trotsenko<sup>2</sup>, D. Banas<sup>2</sup>, F. Bosch<sup>2</sup>, D. Liesen<sup>2</sup>, R. Moshhammer<sup>3</sup>, J. Ullrich<sup>3</sup>, R. Dörner<sup>1</sup>, M. Steck<sup>2</sup>, F. Nolden<sup>2</sup>, H. Rothard<sup>6</sup>, G. Lanza<sup>7</sup>, E. deFilippo<sup>7</sup>

<sup>1</sup>Institut f. Kernphysik, Univ. Frankfurt, <sup>2</sup>GSI-Darmstadt, <sup>3</sup>Max Planck Inst. f. Kernphysik, Heidelberg, <sup>4</sup>Mathematisches Institut, LMU, München, <sup>5</sup>Fudan University, Shanghai <sup>6</sup>CIRIL-Ganil, Caen, France, <sup>7</sup>INFN-Catania-Italy

s.hagmann@gsi.de

**Abstract.** We report on simultaneous measurements of the continuum momentum distribution for RECC cusp electrons and bremsstrahlung in 90 AMeV  $U^{88+} + N_2 \rightarrow U^{88+} + \{N_2^{+*}\} + e_{\text{cusp}}(0^0) + h\nu$  (RECC) collisions. We show that x-ray photons which appear coincident with RECC cusp electrons stem from the short-wavelength limit of the electron-nucleus bremsstrahlung. The observed pronounced asymmetric cusp shape is in good agreement with theory within the relativistic impulse approximation. We expect that when exploiting the full imaging properties of our forward electron spectrometer, fully differential cross sections at the tip region of the bremsstrahlung spectrum with near  $10^{-4}$  electron energy resolution are possible in the near future.

The elementary process of electron nucleus bremsstrahlung has been an important test case for our understanding of the general coupling of electromagnetic fields and matter fields. For low and medium fractional photon energies, i.e.  $E_{h\nu} < 0.5 E_0$  in the bremsstrahlung continuum angular correlations for coincidences between the inelastically scattered electron and the bremsstrahlung photon have exhibited impressive agreement with theory [1]. However, for the high energy region of the bremsstrahlung spectrum, where the electron loses approximately its entire kinetic energy  $E_0$  and a photon with energy  $E_{h\nu} = E_0$  emerges, no differential cross sections of electron-photon coincidences have been reported, even though theory has predicted angular distributions for the coincident scattered electron which are sensitively depending on the direction of the outgoing photon, even when the electron's kinetic energy after the collision is nearly zero [1]. This lack of experiments can be traced to the configuration of standard bremsstrahlung experiments: a fast electron beam is impinging on a thin solid target. Then electrons which have emitted a bremsstrahlung photon and lost nearly their entire kinetic energy cannot escape from the target.

The tip region of the bremsstrahlung spectrum, however, has been nevertheless in the centre of continuous theoretical interest for a variety of reasons: first, it has been experimentally shown that the differential cross section at the short wavelength limit of the bremsstrahlung spectrum is finite for electrons impinging on bare ions[2] ( in contrast to neutral atom as targets). This is physically very plausible as the short wavelength limit in principle is nothing but the transit from free-free to free-bound transitions, e.g L-REC or K-REC for bare ions. The elementary plane wave approximation breaks down in this region and predicts a vanishing cross section; only a theory using point coulomb functions correctly gives the finite cross section. A second reason for the interest is that this region provides the opportunity to theoretically study with the same tools besides bremsstrahlung at once photoionization and its inverse, recombination, and - at high energies - also pair creation.[1-5]. The origin of this occurrence has been associated with the observation by Fano[3,4] and Pratt[5,6] and their co-workers that the region of interest for these processes extends a few Compton wavelengths around the nucleus. Here, however, bound state wave functions and continuum wave functions at the threshold appearing in the pertinent matrix elements are nearly identical. The corresponding differential cross sections are accordingly related by the principle of detailed balancing. Even more, theory predicts that the polarization phenomena in one channel, e.g. bremsstrahlung, will have a close correspondence in another, e.g. photoionization[3,4].

Besides the archetypical experiments carried out in the standard electron atom configuration, electron nucleus bremsstrahlung has also been investigated widely in ion-atom collisions [2,7]. However, only doubly differential cross sections for bremsstrahlung have been reported, where never the emitted electron corresponding to bremsstrahlung photon emission was observed. A number of experiments were executed with swift bare heavy ions impinging on light targets, the bremsstrahlung spectrum thus clearly originating from quasifree target electrons scattered in the projectile field under emission of a photon. In such a situation of inverse kinematics an electron having given up its total kinetic energy  $E_{kin}$  will be found after the collision in the projectile continuum with energy  $\varepsilon' \approx 0$ . This corresponds in the laboratory to the electron transfer from a target atom (at rest) into the projectile continuum cusp with  $\vec{v}_{electron} = \vec{v}_{projectile}$  and a resulting laboratory kinetic energy of the electron  $E_e = (\gamma - 1)mc^2$ , where  $\gamma$  corresponds to the velocity  $\beta$  of the incident projectile  $\gamma = (1 - \beta^2)^{-1/2}$ . From simple kinematics the corresponding bremsstrahlung photon energy at the short wavelength limit observed at  $\theta_L$  in the laboratory frame is

$$E_x^{lab} = \frac{(\gamma - 1)mc^2}{\gamma(1 - \beta \cos \theta^{lab})}$$

For an observer in the laboratory reference frame the radiative process just described is an electron capture to the projectile continuum cusp RECC accompanied by emission of a bremsstrahlung photon. The forward electron cusp observed in swift ion-atom collisions, however, generally contains electrons from other transfer processes as well, that is, cusp electrons not originating in radiative processes like electron-nucleus bremsstrahlung; the non-radiative capture ECC and, for non-bare projectiles, projectile electron loss to continuum ELC are well documented for low collision velocities[9].

It is important to note that except for high collision energies above 20-50 AMeV the non-radiative capture process ECC with identical initial and final states of the collision partners has been theoretically predicted to have a larger cross section than the RECC channel and will dominate the total electron cusp cross sections.

It is the goal of the present experiment to explore the feasibility to study the elementary process of electron nucleus bremsstrahlung at the short wavelength limit in inverse kinematics via ion-atom collisions even in the presence of strong non-radiative capture to continuum channels.

#### Experimental Procedure

We will shortly describe the experimental set-up; a detailed description is given elsewhere [11]. The experiment was performed at the supersonic gas target of the GSI experimental storage ring ESR. Only this facility can provide projectile beams with high nuclear charge up to  $Z=92$  in very high charge states  $q$  over a very wide velocity range with the brilliance[7] necessary for coincidence experiments. Here U-ions with a specific energy of 90 AMeV ( $\gamma=1.0966$ ,  $\beta=0.4104$ ,  $E_{cusp}=49.36$  keV) and in a selected charge state 88+ are injected into the ESR. The  $U^{88+}(1s^2 2s^2)$  beam conveniently facilitates tuning of the electron spectrometer during set-up using the strong electron loss to continuum (ELC) cusp.

X-rays emerging from the interaction region are detected at  $90^\circ$  with respect to the beam axis with a 2000 mm<sup>2</sup> HPGe x-ray detector subtending a solid angle of  $8 \cdot 10^{-3}$  at an angular acceptance of  $\pm 9.4^\circ$ ; the energy resolution

of the x-ray detector is 900 eV at 59.5 keV. Electrons emitted in the forward direction at  $0^\circ \pm 1.9^\circ$  are separated from the coasting beam by a  $60^\circ$  dipole magnet downstream of the target zone, the geometric solid angle is  $1.1 \cdot 10^{-3}$  of  $4\pi$ . This magnet is the first optical element of the imaging forward electron spectrometer, consisting of a  $60^\circ$  dipole, a quadrupole triplet and a second  $60^\circ$  dipole. Following momentum defining slits electrons are detected with a channel plate detector equipped with a 2D position sensitive delay line anode.

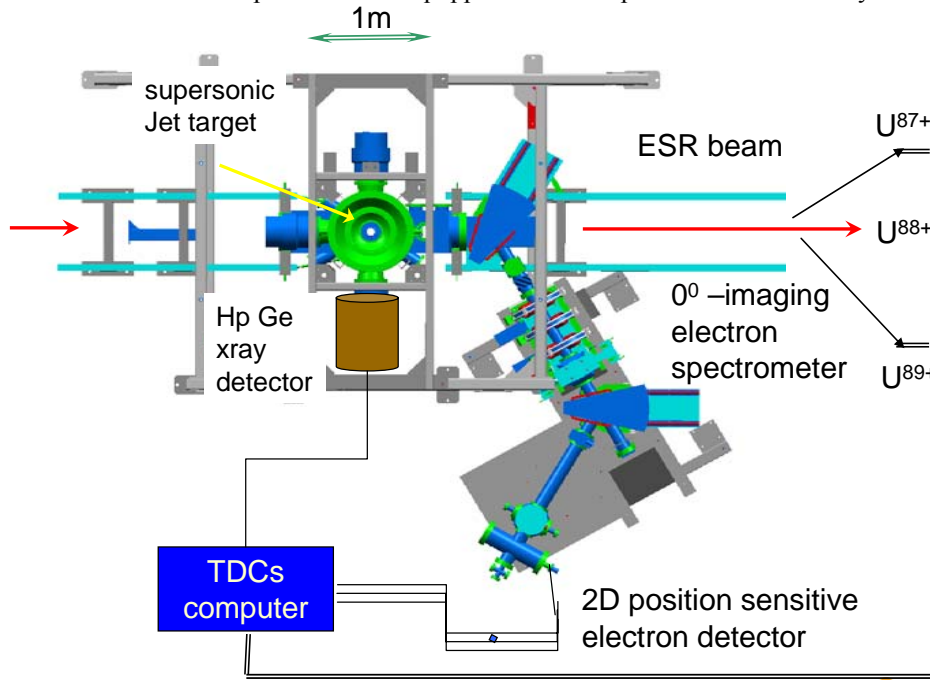
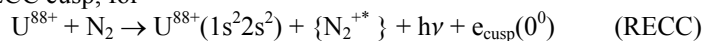


Fig. 1: Experimental set-up including the forward electron spectrometer and the x ray detector at the supersonic jet-target zone of the ESR. The interception of the projectiles having captured or lost an electron is indicated as well as the integration of their detection signals into the experimental configuration.

Relative double differential cross sections for forward electron production are measured by incrementing the electron spectrometer's B-fields after a predetermined number of fillings of the ESR. Although we report only on doubly differential cross sections we are bound to perform coincidence measurements because at the collision velocity of interest the non radiative ELC and ECC prevail [10a,11] over the radiative RECC. This causes the ELC and ECC electron cusps to dominate the measured non-coincident spectrum.

#### Results and Discussion

In fig 2 we show the double differential cross section for radiative electron capture to the projectile continuum, i.e. the RECC cusp, for



has been derived as a function of the electron momentum in the laboratory frame from coincidences between x-ray photons detected under  $\theta=90^\circ$  and electrons analyzed using the forward electron spectrometer. The DDCS exhibits a cusp at  $\vec{v}_{\text{electron}} = \vec{v}_{\text{projectile}}$  which coincides with the simultaneously measured ELC and the Coulomb capture ECC [11] cusp maxima. The DDCS for the ELC is acquired via coincidences of forward electrons with the charge changed  $U^{89+}$  beam intercepted downstream of the target area. The relative cross section for the ECC is derived from appropriate subtraction of electrons coincident with both charge exchanged beam components and x rays, respectively. Details of the simultaneous measurement of the DDCSs for RECC, ELC and ECC channels will be given in a forthcoming publication [12].

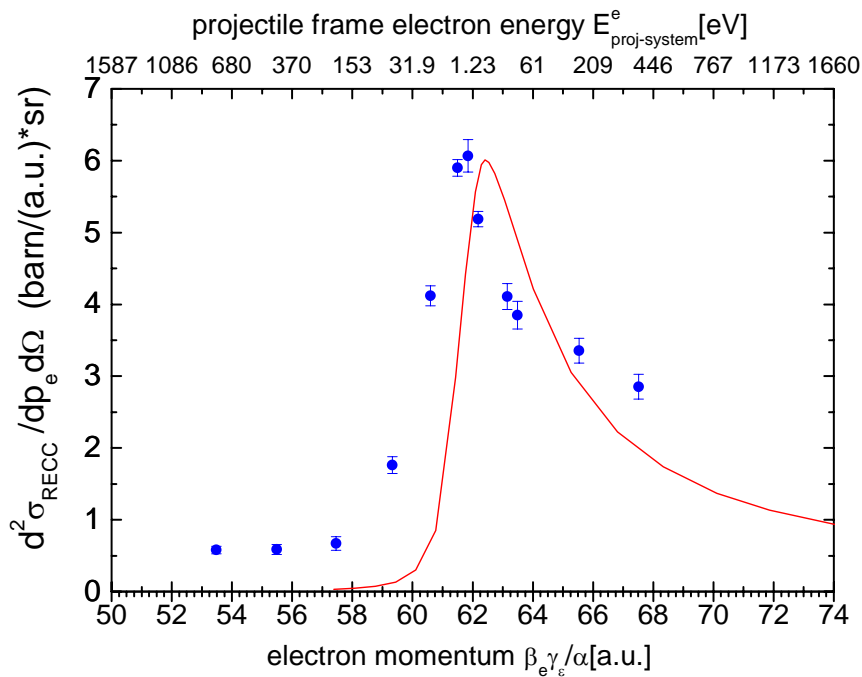


Fig. 2 Double differential cross section (DDCS) for radiative electron capture to the continuum (RECC) presented as a function of the laboratory electron momentum  $\beta\gamma/\alpha$  in a.u. (lower scale). The abscissa on the top corresponds to the electron kinetic energy in the projectile frame  $E_{\text{proj.system}}^e$ . The relation between laboratory electron momentum  $\beta\gamma/\alpha$  and projectile frame electron energy  $E_{\text{proj.system}}^e$  is highly non-linear. The zero for  $E_{\text{proj.system}}^e$  occurs for  $\beta\gamma/\alpha = 61.67$  a.u. which corresponds to an electron travelling with projectile velocity. The full curve represents the theoretical DDCS folded with the instrumental momentum resolution. The experimental cross section is normalized to the maximum of the theoretical DDCS.

The pronounced peak asymmetry of the RECC cusp emphasizes the high energy slope of the cusp; this is well described by the relativistic impulse approximation. The asymmetry is opposite to the one found for Coulomb capture (ECC) at lower collision energies[8,9] and may be understood as follows: For an observer in the  $U^{88+}$ -projectile frame the incident target electron is decelerated from  $v_{e-ps} \approx v_{\text{proj}}$  to a velocity  $\approx 0$ , its total kinetic energy being carried away by the x-ray photon. With nearly its complete kinetic energy transferred to the photon the electron remains with very little kinetic energy  $E_{\text{proj.system}}^e$  in the projectile frame, bounces back from the projectile and, thus, appears – now seen in the laboratory reference frame - predominantly in the beam direction with corresponding momentum  $p_e > \beta\gamma/\alpha$  [10b]. It is interesting to compare with the non-radiative ECC channel: in the ECC process the cusp electrons originate from quasielastic scattering of high momentum components of the target from the projectile. As it is well known that elastic scattering favours forward angles, it is easily seen that the corresponding ECC electrons are predominantly emitted antiparallel to the beam direction[10b] leading to the well known asymmetry, now on the low momentum side of the ECC cusp.

Comparison is made with RECC calculations using the relativistic impulse approximation [10b]. This theory can be interpreted as a convolution of the Elwert-Haug bremsstrahlung theory [1] with the momentum distribution of the initial electronic state, and is described in [10]. The experiment is normalized to theory at the cusp maximum. The full curve in fig. 2 represents the theoretical DDCS (with its divergence at  $\vec{v}_{\text{electron}} = \vec{v}_{\text{projectile}}$ ) folded with the instrumental momentum resolution  $\Delta p/p = 1.9\%$ . The theory is in addition averaged over the angular resolution of the electron detector and integrated over the acceptance of the photon detector. Since the latter

implies integration over the target Compton profile, the different subshell contributions differ at most by 5% for the high collision energy considered here (note, the N<sub>2</sub> target has been used for technical reasons, since a considerably denser target can be provided at the internal ESR jet for N<sub>2</sub> than for H<sub>2</sub>).

We observe that the maximum of the theoretical DDCCS for RECC occurs at a slightly higher electron laboratory momentum than the experimental maximum. In fact, this shift of the theoretical curve away from the "true" cusp position  $\vec{p}_0$  is due to the folding procedure. The asymmetric shape function S of the theoretical DDCCS with its true maximum centred at  $\vec{v}_{electron} = \vec{v}_{projectile}$  is shifted into the direction of the gentler slope of S, i.e. in the direction of higher electron momenta, if folded with a resolution function R. The comparison of experimental and theoretical cusp shapes is complicated, however, by a contribution appearing in the experimental DDCCS that is not accounted for by theory: it originates from electrons captured into Rydberg states of the projectile and subsequently field ionized in the 60° magnet. This supplemental part of the electron spectrum is centred at  $\vec{v}_{electron} = \vec{v}_{projectile}$  and is not shifted by folding with R; its inclusion in a theoretical calculation, not consistently feasible within the present approach, would tend to reduce the difference between the experimental and theoretical peak positions.

The x-ray spectra coincident with the electrons from the cusp impressively confirm the interpretation of RECC as the inverse bremsstrahlung at the short wavelength limit (viewed by an observer in the projectile system). In fig. 3 we compare the x-ray spectrum coincident with electrons from the cusp peak at  $v_{elec}=v_{proj}$  with a non-coincident x-ray spectrum which has been scaled down for convenience of comparison. While the non-coincident spectrum is dominated by characteristic projectile M- and L- x-ray emission, the coincident spectrum almost exclusively contains x-rays at  $E_x \approx 45$  keV. This energy coincides with the (laboratory frame) short-wavelength limit of electron-nucleus bremsstrahlung  $E = (\gamma - 1) mc^2 \gamma^{-1} (1 - \beta \cos \theta)^{-1}$  from  $e^- + U^{88+}$  at  $(\gamma - 1)mc^2 = 49.4$  keV incident kinetic electron energy and  $\theta = 90^\circ$  x-ray observation angle. Also shown is the calculated photon spectrum obtained from the fourfold differential cross section by integrating over the forward electron acceptance cone and the energy resolution of the spectrometer. Theory is normalized to experiment in the peak maximum to show the good representation of the experimental peak width by theory.

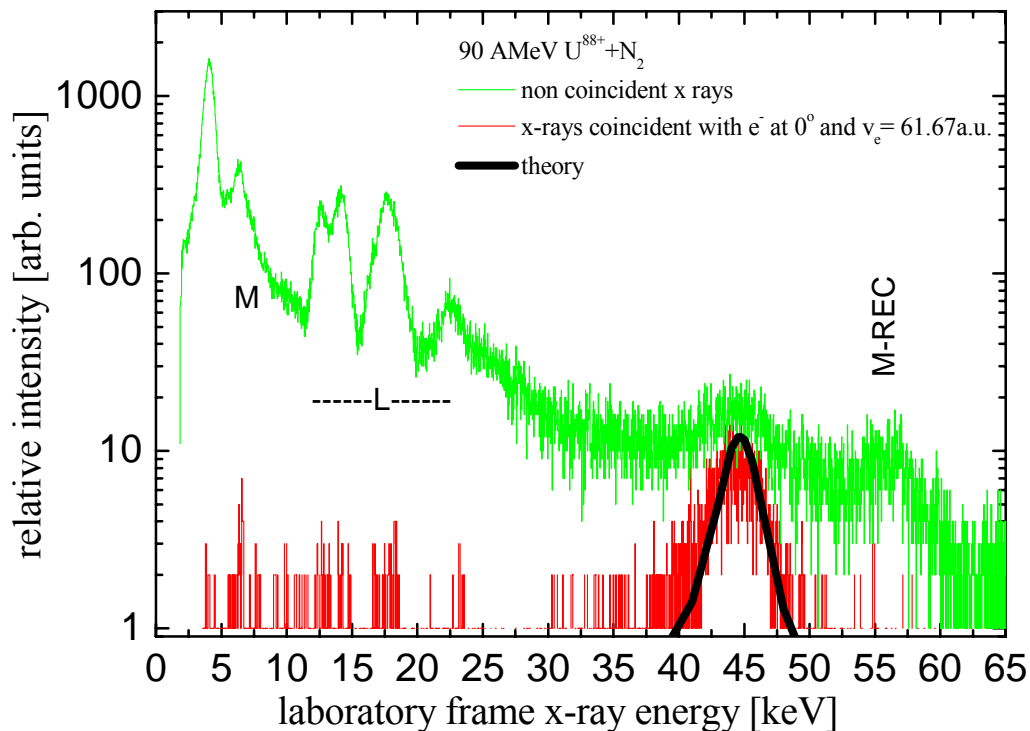


Fig. 3 X-ray spectrum coincident with RECC electrons compared with a singles x-ray spectrum detected at  $\theta = 90^\circ$  with respect to the beam axis and with relativistic impulse approximation theory. The width of the x-ray

*peak is mainly given by the resolution function of the photon detector. The range of the characteristic U L- and M- x rays is indicated.*

#### Summary

We have measured for the first time coincidences between electrons from the RECC cusp and bremsstrahlung at  $90^\circ$  for 90 AMeV  $U^{88+} + N_2$  collisions. We have confirmed the interpretation of RECC electrons as originating from the fundamental process of electron-nucleus bremsstrahlung at the short-wavelength limit. There is a satisfactory agreement between experiment and theory with respect to the principal features in the cusp electron and coincident photon spectra. A comparison on an absolute scale is deferred to future work. We note that with a configuration where all pertinent momenta are determined – e.g. using a reaction microscope in addition to a 2D position sensitive detector for cusp electrons, – the measurement of fully differential cross sections for the short-wavelength limit of electron nucleus bremsstrahlung with near  $10^{-4}$  energy resolution will become feasible. This will provide for sensitive experimental tests of the usual approximations made in the theoretical treatment (like the impulse approximation).

#### Acknowledgment.

We gratefully acknowledge financial support by the GSI F&E program, the Bundesministerium für Forschung und Technologie BMBF, the Max Planck Gesellschaft MPG and the Deutsche Forschungsgemeinschaft DFG.

#### References:

1. E. Haug, W. Nakel, The Elementary Process of Bremsstrahlung, World Scientific Lecture Notes Vol. **73**(2004)
2. T. Ludziejewski et al., J. Phys. **B31**, 2601(1998), Hyp. Inter. **114**, 165(1998)
3. U. Fano et al., Phys. Rev. **116**, 1147, 1156, 1159(1959)
4. U. Fano et al., Phys. Rev. **112**, 1679(1958)
5. R. Pratt et al., Phys. Rev. **120**, 1717(1960), Phys. Rev. **A11**, 1797(1975)
6. R. Jabbur et al., Phys. Rev **129**, 184(1963)
7. A. Gumberidze et al., Phys. Rev. Lett. **94**, 223001(2005)
8. D. Jakubassa in Lecture Notes in Physics, Vol. **213**, p 17(1984), Springer, Heidelberg
9. J. Burgdörfer in Lecture Notes in Physics, Vol. **213**, p 32(1984) Springer, Heidelberg
10. a) D. H. Jakubassa-Amundsen, Eur. Phys. J. **D41**, 267 (2007)  
b) D. H. Jakubassa-Amundsen, J. Phys. **B36**, 1971(2003); in the literature RECC is also called RI= radiative ionization
11. M. Nofal, Diss. Univ. Frankfurt (2007) and M. Nofal et al. Phys. Rev. Lett. ( in print)
12. M. Nofal et al. to be published